

N76-28274

A MOBILE PLANETARY LANDER UTILIZING
ELASTIC LOOP SUSPENSION

By W. Trautwein

Lockheed Missiles & Space Company, Inc.
Huntsville Research & Engineering Center

ABSTRACT

Efforts to increase the cost effectiveness of future lunar and planetary rover missions have led to the mobile lander concept, which replaces the landing legs of a soft-lander craft with a compact mobility system of sufficient strength to withstand the landing impact. The results of a mobile lander conceptual design effort based on existing NASA-Viking '75 hardware are presented. The elastic loop concept, developed as a post-Apollo rover technology, is found to meet stringent stowage, traction, power and weight requirements.

INTRODUCTION

Future rover missions to the moon or to Mars must promise exceptional returns on the investment in order to successfully compete for funding in the constrained fiscal environment of the years ahead.

Mars exploration will intensify dramatically in mid-1976 when two stationary NASA-Viking spacecraft are expected to soft-land on the red planet and perform biological, photographic, geological and meteorological experiments at their landing sites. However, such localized spot checks can only scratch the surface of exploring a planet. The question arises: What type of follow-on mission will provide the highest and most cost effective scientific return after the first successful soft landings at isolated sites?

Through early 1974 NASA inhouse studies (Ref. 1) as well as several industry projects by Martin-Marietta Corporation (MMC) (Ref. 2) and by Messerschmitt-Boelkow-Blohm (MBB) (Ref. 3) pointed toward additional lander missions incorporating a small roving vehicle that would be stowed on top of and deployed from a slightly modified lander craft. The existing Viking Mars Lander and its entry capsule can accommodate four-wheeled rovers of 120 to 180 cm length and wheel diameters of 48 to 56 cm, where the larger size rover would require folding hinges for stowing the chassis inside the existing Viking capsule. A medium rover of 100 kg mass (Ref. 2) and an autonomous rover of 180 kg mass were studied in some depth (Ref. 3).

NASA estimates of the development cost of a piggyback rover were \$80 million, which is considered to be too high for funding in the near future in view of the present constrained fiscal environment. Efforts to win the participation of the European Space Research Organization in a cost-sharing program for rover development were not successful.

THE MOBILE LANDER CONCEPT

Background and Basic Design Features

In efforts to improve the cost-effectiveness of planetary rovers, the Martin-Marietta Corporation (MMC) reexamined the idea of a mobile lander after earlier studies to mobilize the entire Viking Lander by conventional wheels had shown negative results (Ref. 4). NASA's Marshall Space Flight Center (MSFC), which was responsible for the Apollo Lunar Roving Vehicle development, was consulted by MMC in a search for lightweight wheels, tracks or rollers of high flotation. NASA-MSFC recommended use of elastic loops, which had been developed by Lockheed Missiles & Space Company in Huntsville under partial NASA-MSFC sponsorship for post-Apollo rover missions (Refs. 5 and 6). In design studies performed by Lockheed during the summer of 1974 in cooperation with MMC under NASA guidance the feasibility of mobilizing an entire Viking lander with minimum modifications to the lander and entry system was demonstrated. A candidate Viking mobile lander configuration is shown in Figure 1.

The lander's landing pads are replaced by a pair of elastic loops at the front (Figure 2) and single elastic loops at each rear leg. The elastic loop suspensions consist of one-piece self-supporting bands of high strength material and provide a large ground contact area with minimum stowage requirements. Their advanced state of development played a vital role in making the mobile lander concept credible. The following design guidelines had been established:

- The mobility system will attach to a landing gear similar to that of the current Viking '75 Lander and will be stowable in the volume available within the Viking '75 entry capsule.
- The mobility system will be deployed by the landing gear system.
- The lander craft will land on the mobility system. Landing loads will be transmitted through the carriages of the mobility system, which will be protected from the initial touchdown shock by shock absorbing pads.
- The ground contact area of the operational mobility system will be sufficient to limit sinkage in Martian loess material to 4 cm.
- The mission duration after landing will be 180 days.
- The mobility system will be designed for a range of 150 km and for night and day operation (temperature extremes $-84^{\circ}\text{C} \leq T \leq +65^{\circ}\text{C}$).

The development cost for a mobile lander based on an existing stationary lander craft has been estimated to be only one third of the cost of an autonomous "piggy-back" roving vehicle. A mobile Viking Lander mission has therefore been endorsed by NASA's Director of Planetary Programs as the logical next step in Mars exploration after the 1976 Viking landings (Ref. 7).

In the following sections major results of LMSC's design effort on a Mobile Lander based on the existing Viking landing craft will be summarized.

MOBILITY SYSTEM DESIGN

Selection of Concept

Since the mobility system of a mobile lander should fit within the aeroshell of an existing lander craft and take up not much more space than the landing legs which it replaces, compact stowage is the major design requirement. However, the ground contact area must be sized to ascertain sufficient traction and acceptable sinkage in the worst type of expected soil conditions. In a comparison of stowage volume, weight and mechanical complexity of wheels, tracks and elastic loops for specified footprint requirements, elastic loops and tracks are found to be substantially more compact than wheels. Elastic loops have the further advantage of lighter weight, simpler design and lower internal power losses over tracks as was demonstrated in NASA-sponsored prototype development and test programs (Refs. 5 and 8). A small three-loop test vehicle (Figure 3) built by Lockheed for NASA-MSFC demonstrated excellent rough-terrain mobility in soil bins and on obstacle courses. Yaw steering of the single loop, augmented in tight turns by differential speed control of the other loops, was found to provide good energy-saving steering response. A three-loop configuration with yaw steering of the front loop was therefore selected for the preliminary design. The three-legged Viking lander represented a perfect match for this configuration.

Loop Sizing

Extensive performance tests of elastic loop prototypes at MSFC's Wheel-Soil Interaction Test Facility and at the U.S. Army Engineer Waterways Experiment Station (Ref. 8) in lunar soil simulant provide a reliable basis for loop sizing. Loop sizes which satisfy the footprint requirements for the maximum landed mass of a 1979 Viking mission and yet allow stowage within the existing Viking entry capsule are listed in Table 1.

The penalty in weight, complexity and tractive efficiency of a dual-loop configuration could be justified for the front leg, which favors a short pair of loops for stowage and for yaw steering. For the rear legs, which do not require yaw steering, single loop support is more attractive.

Loop Fatigue Considerations

The two 180-degree sections of an elastic loop must provide sufficient bending stiffness to support the load without excessive deformations. Approximate stress-deformation formulas were derived based on a simplified theory which treats deformations of the transversely curved loops as inextensional bending distortions.

The specific loop strength is primarily dependent upon the flexural fatigue strength σ_f of the loop material evaluated for the required number of load cycles (2.3×10^5 cycles over 150 km range). Of several candidate loop materials glass fiber reinforced epoxy and titanium alloy ranked

highest in specific strength. Glass-epoxy composite material appears best suited for minimum weight loops. An experimental glass-epoxy loop for a 3300 N design load of only 11 kg mass is shown in Fig. 5 during fatigue testing in a moving belt dynamometer (Ref. 12). In order to minimize the amounts of organic material on the Viking Lander because of possible interference with the biological experiments, the high strength titanium alloy Beta III was chosen. Its specific fatigue strength is 76% of S-Glass epoxy. The manufacture of seamless loops by roll extrusion of forged ring blanks and subsequent hot forming was found feasible.

Loop Stowage, Deployment and Protection from Landing Impact

A candidate concept for loop stowage and deployment which is compatible with the existing Viking '75 aeroshell contours and the Viking '75 main strut is shown in Figures 2 and 4. The two front loops are sandwiched between the carriage bottom and a landing pad (Figure 4a) to prevent local deformations during the landing impact. By depressing the upper loop sections the stowed length is minimized and sufficient roll capability ± 19 deg) is achieved for the carriage to adapt to the maximum expected slopes during touchdown without interference between loops and struts. Under the maximum expected landing loads the main strut will be compressed to the position shown in Figure 2 for the operational loops, which leaves at least 28 cm ground clearance. Upon separation of the landing pads after landing the loops will snap into their operational form with straight upper and lower sections. The front idler sprockets will swing forward and maintain permanent contact with the loops.

The energy absorbing landing pads have been designed to surround the lower loop sections completely during landing. Furthermore, the bottom surface of the carriage is contoured to closely match the loop shape in the stowed position as shown in Figure 2. The Viking '75 landing leg design loads are based on 200 g maximum vertical deceleration of the landing pads, which is attenuated by the main struts to a maximum of 30 g for the lander chassis by crushable honeycomb cartridges inside the main struts.

The preliminary landing pad design is based on the worst case conditions illustrated in Figure 6 (provided by R. J. Muraca, NASA-Langley). The face sheets at the bottom of the landing pads were assumed to distribute point loads from rock impact over an area $A_r = 470 \text{ cm}^2$. The main strut force versus stroke characteristics indicate that the average crush force during the initial phase of the landing impact is $F_a = 4450 \text{ N}$. The total energy to be absorbed by the landing pad to decelerate the mass m_{l3} of leg 3 (below main strut No. 3) is then

$$(1) \quad E_3 = 1/2 m_{l3} v_0^2 + F_a x_p,$$

where x_p is the stroke of the crushable landing pad. Neglecting the small initial energy absorption in the main strut during the force buildup to F_a , all energy absorption then occurs in the landing pad with crush strength p or

$$(2) \quad E_3 = A_r p x_p.$$

Substituting (2) into (1) and solving for the required crush stroke yields for $m_{\ell 3} = 15.4$ kg:

$$(3) \quad x_p = 1/2 m_3 v_o^2 / (A_r p - F_a) = 4.2 \text{ cm} .$$

The allowable crushing stroke is 70% of the pad's thickness. The required honeycomb thickness is therefore $x_{hc} = 4.2/0.7 = 6$ cm. The maximum deceleration is encountered for a flat landing with uniform crushing of the full pad area. The selected crush strength and pad area must be sufficiently low to limit the deceleration to 200 g. The maximum allowable pad area A_o can be determined as follows: the maximum allowable pad load is $F_o = m_{\ell 3} g_{max} + F_a = 34.65$ kN. For the selected honeycomb material with crush strength $p = 24.1$ N/cm² the pad area should be $A_o \leq F_o/p = 1438$ cm². However, the projected pad area for full protection of both front loops is $A_1 = 1768$ cm². Therefore the honeycomb must be "checkerboarded" leaving $A_1 - A_o = 330$ cm² of voids or a slightly softer honeycomb material must be found. Similar approximate calculations led to a required lateral pad thickness of 0.9 cm to protect the loops from side impact loads.

Drive System and Power Requirements

The drive system design requires trade studies between light weight and safe lubrication at the low temperature extremes. The present state of the art in bearing and gear lubrication requires dry lubricants for safe operation at -84°C. Since direct drive torque motors were ruled out due to heavy weight, brushless dc motors with gear reducer were chosen as primary candidates for further study. The gear ratio was chosen to limit the motor revolutions to 11 million over the operational life of the drive system. A 30:1 high efficiency roller-gear reduction was selected, which forms an integral part of the drive sprocket together with a brushless motor with parking brake and an emergency disconnect clutch. The weight of the complete drive sprocket/motor/gear/brake assembly is estimated at less than 3.5 kg.

Extensive performance tests of elastic loop prototypes at NASA-MSFC and at the U. S. Army Engineer Waterways Experiment Station (WES) (Ref. 8) provide a sound data base to predict power requirements. The Lunar Soil Simulant in the loose air dry test condition is very close to the assumptions made for Martian loess. The tests were performed for a wide range of slope angles up to 38 deg. Test results are documented in normalized form in Ref. 8 and can be readily applied to specific vehicle characteristics. For the mobile Viking Lander's weight on Mars of $W = 2510$ N the power requirements plotted in Figure 7 are predicted.

COMPARISON OF ROVER AND MOBILE LANDER MOBILITY CHARACTERISTICS

During development of the 4-wheeled Lunar Roving Vehicle (LRV) extensive performance tests of wiremesh wheels had been conducted at the

Waterways Experiment Station (WES) in Lunar Soil Simulant (Ref. 9). Since the majority of the elastic loop tests were performed in the same facility in identical soil conditions, the test results obtained for both concepts can be directly compared.

Slope Climbing Capability

In Figure 8 (taken from Ref. 8) specific energy and slope climbing ability are plotted for the LRV wheel and an elastic loop test unit tested in identical soft Lunar Soil Simulant. Between 0 and 10 deg slope angle wheels are found to require 30% more energy than elastic loops. For steeper slopes wheel performance rapidly deteriorates even more. The wheels spin out at 20 deg slope angle whereas elastic loops climb slopes up to 36 deg in this soft soil with propulsive efficiency peaking near 30 deg ($\eta_{\max} = 80\%$). For a moderate 10 deg slope the efficiencies of wheels and elastic loops are 45 and 63%, respectively. This superior soft soil performance of elastic loops can be attributed to the reduced sinkage, reduced slip and more uniform pressure distribution. The excellent traction of the loops not only improves slope climbing but also adds maneuverability by good response to pivot steering and braking commands.

Static Stability

Piggyback rovers are constrained in wheelbase and treadwidth by the limited stowage space on top of the lander craft. Even the additional complexity of a hinged chassis as proposed for the MBB rover (Ref. 3) results in vehicle dimensions which are substantially smaller than those of a mobile lander. These differences in vehicle geometry are reflected in the static stability limits plotted in Figure 9 for varying slope angles and assuming an additional rock under the uphill wheels (or loop). The three widely spaced lander legs provide exceptional static stability in roll, which, in general, is more critical than pitch stability.

Obstacle Negotiation

Good obstacle climbing capability is a key factor in reducing the risk of mission failure in an automated rover mission when unforeseen hazards are encountered. Furthermore, exceptional obstacle performance reduces the time and energy required to safely reach a given destination because minor obstructions can be negotiated without bypass maneuvers. The obstacle climbing of four-wheeled vehicles has been investigated in depth by Kuehner (Ref. 10) and more systematically by Rettig and Bekker (Ref. 11).

Vertical Obstacle Climbing

For all four-wheeled vehicles with all wheel drive and near uniform load distribution the rear wheels limit the vertical step negotiation. In the limiting condition (Fig. 10) the weight W , tangential and normal forces at front and rear wheels are in equilibrium. For small chassis pitch angles β this results in the following equation

$$(4) \quad [(1 - \mu\beta) + \mu\lambda] \sin\alpha - \left[\gamma - \mu + \left(\gamma \frac{h_o}{s} - 1 \right) \beta + \lambda \right] \cos\alpha = \mu \lambda$$

where $\lambda = D/2s$, $\gamma = (1 + \mu^2)^{1/2} s_1 / \mu s$, which must be solved for α and β , since $\alpha = \arcsin(1-2h/D)$ and $\beta = \arcsin(h/s)$ are functions of the wanted obstacle height h . For the piggyback rover proposed by MBB (Ref. 3), Eq. (4) yields a maximum vertical step height (assuming $\mu = 0.6$) of $h = 8.1$ cm ($\alpha = 41.5$ deg; $\beta = 5.2$ deg), whereas the solution for the smaller rover proposed by MMC (Ref. 2) is $h = 5.7$ cm ($\alpha = 51.3$ deg; $\beta = 5.4$ deg), which must be considered insufficient in view of the poor knowledge about martian surface details.

Obstacle heights of $h = 26$ cm were claimed in Ref. 3 without proof for both rover designs. NASA-sponsored obstacle climbing tests with the three-loop configuration of Figure 3 have shown (Ref. 5) that three-loop vehicles with pitch articulated loop suspensions as proposed for the mobile lander can climb obstacles which are 64 and 85% of the loop length in forward and reverse direction (single loop trailing), respectively. Reducing these test results from the test conditions ($\mu = 0.8$) to the assumed martian soil conditions ($\mu = 0.6$) the step heights decrease by 28% based on the analytical and experimental results in Ref. 5. In forward and reverse direction obstacle performance is limited by the rear loop pair. For the present length of the rear loops ($L = 63$ cm) the maximum step heights: $h_{\text{fwd}} = 0.72 \times 0.64 \times 63 = 29$ cm; $h_{\text{rev}} = 0.72 \times 0.85 \times 63 = 39$ cm result, which in the forward direction is consistent with the planned ground clearance of 28 cm and allows for safe negotiation of 22 cm high rocks expected in the landing area.

The major mass, size and performance data of the mobile lander and piggyback rovers are summarized in Table 2.

CONCLUSIONS

The compact size, light weight and large footprint of elastic loop suspensions was found to offer surface mobility for an entire planetary soft lander of the Viking class without major modifications of lander or entry system hardware. Compared with recent "piggyback" Mars rover designs the scientific value of a mobile lander mission is greatly enhanced because the complete science payload is mobile and the full power, communications, data processing and thermal resources of the lander are available for the science instruments. The larger vehicle dimensions add stability and obstacle climbing capability. Expected development cost is lower because most existing Viking subsystems including scientific instruments, cameras, communications, data, storage and handling and thermal control systems can be used without modifications while a piggyback rover requires separate subsystems, which for the most part will differ from the existing lander versions. The low weight required for lander mobilization should make the mobile lander concept very attractive for a Mars sample return mission, since more than one geological and ecological environment can be sampled, thereby greatly enhancing the scientific value of the samples collected for return to earth.

REFERENCES

1. Darnell, W. L., and Wessel, V. W., Conceptual Design and Operational Characteristics of Mars Rovers for Advanced Viking Science Missions NASA-Langley Working Paper 1113, June 1973.
2. Martin-Marietta Corporation, Viking '79 Rover Study Final Report. Summary Report, Vol. I, NASA-CR-132417, Detailed Tech. Rep., Vol. II, NASA-CR-132418, March 1974.
3. Koelle, D. E., Kokott, W., and Schultze, W., A Mars Rover Concept for Future Landing Missions, Raumfahrtforschung 18 (1974), pp. 224-235.
4. Martin-Marietta Corporation, Study of Application of Adaptive Systems to the Exploration of the Solar System, NASA-CR-132258, Vol. III, March 1973.
5. Costes, Nicholas C., Melzer, K-J., and Trautwein, Wolfgang, Terrain-Vehicle Dynamic Interaction Studies of a Mobility Concept (ELMS) for Planetary Surface Exploration, AIAA Paper No. 73-407, March 1973.
6. Costes, N. C., and Trautwein, W., Elastic Loop Mobility System - A New Concept for Planetary Exploration, J. of Terramechanics, Vol. 10, No. I, (1973), pp. 89-104.
7. Kraemer, R. S., Planetary Missions: Making Do, J. of Astronautics & Aeronautics, November 1974, pp. 10-12.
8. Melzer, K-J., and Swanson, G. D., Performance Evaluation of a Second Generation Elastic Loop Mobility System, Tech. Rep. M-74-7, U. S. Army Engineer Waterways Experiment Station, June 1974.
9. Green, A. J., and Melzer, K-J., Performance of Boeing LRV Wheels in a Lunar Soil Simulant, U. S. Army Engineer Waterways Experiment Station, Tech. Rep. M-71-10, December 1971.
10. Kuehner, K., Das Kraftfahrzeug Im Gelaende, ZVDI, 79 (1935) pp. 1019-1027.
11. Rettig, G. P., and Bekker, M. G., Obstacle Performance of Wheeled Vehicles, U. S. Army OTAC Rep. No. 29, 1958.
12. Trautwein, W., G. W. Fust, and J. A. Mayhall, Exploratory Development of Loopwheel Suspensions for Off-Road Military Vehicles, Final Report, Part 1, Contract N61331-74-C-0064, Material Selection and Structural Test Loop Design, Lockheed Missiles & Space Company, Huntsville, Ala., July 1974; Part 2, Contract N-61339-75-C-0090, Loop Core Fabrication and Testing, Lockheed Missiles & Space Company, Huntsville, Ala., December 1975.

Table 1. Loop data for dual- and single-loop support of Viking lander legs

Configuration	Overall loop		Ground Contact Pressure N/cm ²	Loop thickness mm	Vertical Spring Rate ^a N/cm	Mass ^b kg
	Length cm.	Width cm				
Two loops/leg	55	17	0.45	1.47	72	5.22 (2 loops)
One loop/leg	63	27	0.49	1.88	66	5.46 (1 loop)

^aBased on 675 kg supported mass on Mars uniformly distributed over three legs.

^bMass of loop(s) required per leg, including inner drive lugs and outer grousers. Loop material: Titanium alloy Ti-4.5Sn-5Zr-11.5Mo (Beta III).

Table 2. Summary of major size, mass and performance characteristics of rover and mobile lander designs compatible with Viking aeroshell

	Piggyback rover designs by		Mobile lander design
	MMC (Ref. 2)	MBB (Ref. 3)	
Wheel base	60 cm	90 cm ^a	205 cm
Tread width	60 cm	94 cm ^a	235 cm
Total mass	108 kg	180 kg	675 kg
Mass of mobility system			50 kg
Mobile science payload	21 kg	55 kg	100 kg
Ground pressure	0.5 N/cm ²	0.75 N/cm ^{2b}	0.47 N/cm ²
Ground clearance	22 cm	25 cm	28 cm
Max. obstacle height for $\mu = 0.6$	5.7 cm ^c	8.1 cm ^d	29 cm forward 39 cm reverse
Max. slope angle in Soft Soil Simulant ^e	20 deg	20 deg	36 deg

^aChassis requires folding for stowage inside Viking capsule.

^bConsidered too high for safe soft soil mobility.

^cCan be improved to 12.4 cm by forward shift of c.g. to $s_1/s = 0.35$; however, front ground pressure then is 85% higher than rear.

^dCan be improved to 13.2 cm in same way and with same penalty as (c).

^eBased on NASA-sponsored soil bin tests (Refs. 8 and 9).

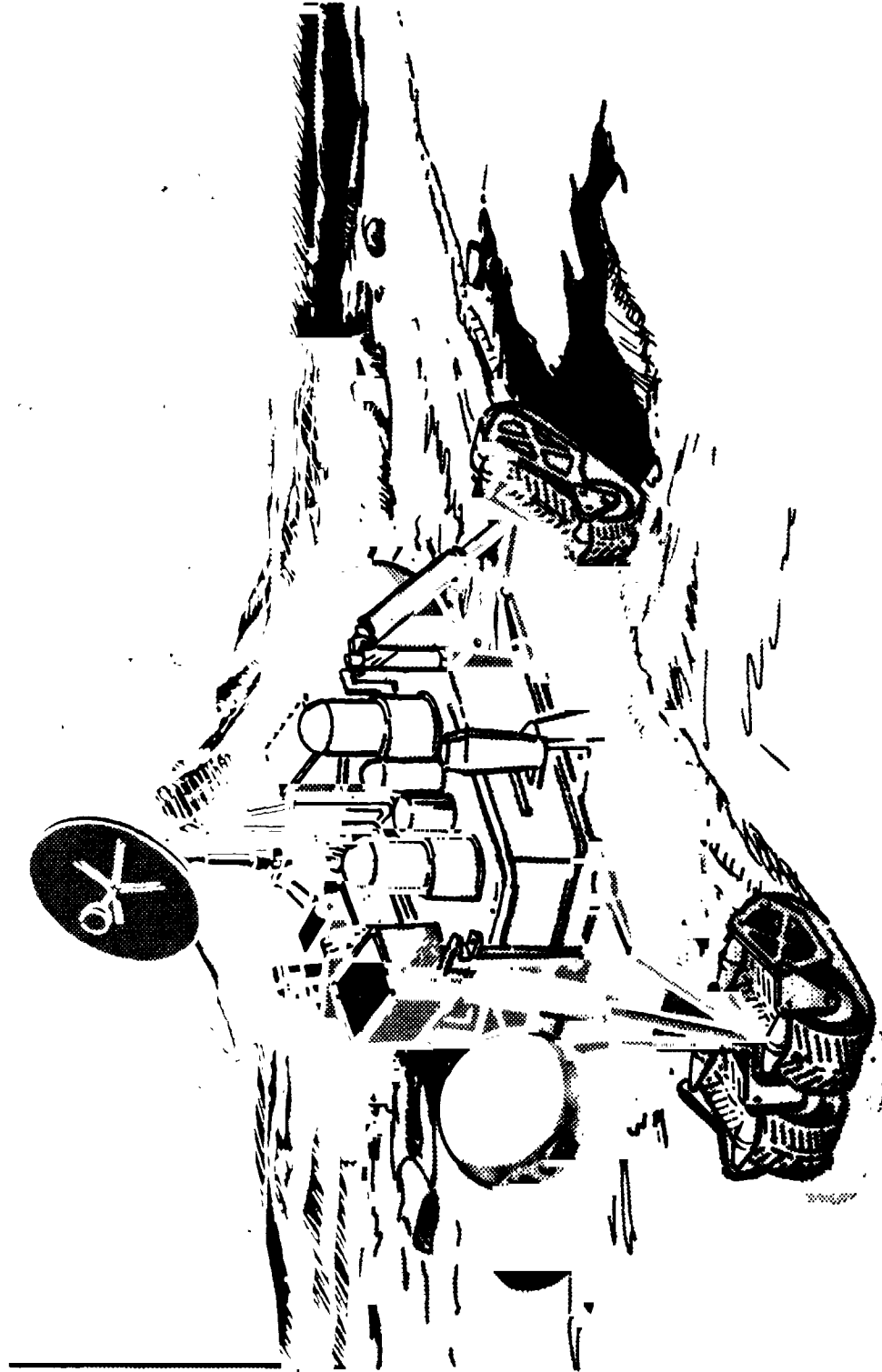


Fig. 1 - Candidate mobile Viking Lander configuration. A pair of steerable elastic loops supports front leg. Rear legs are supported by longer single loops.

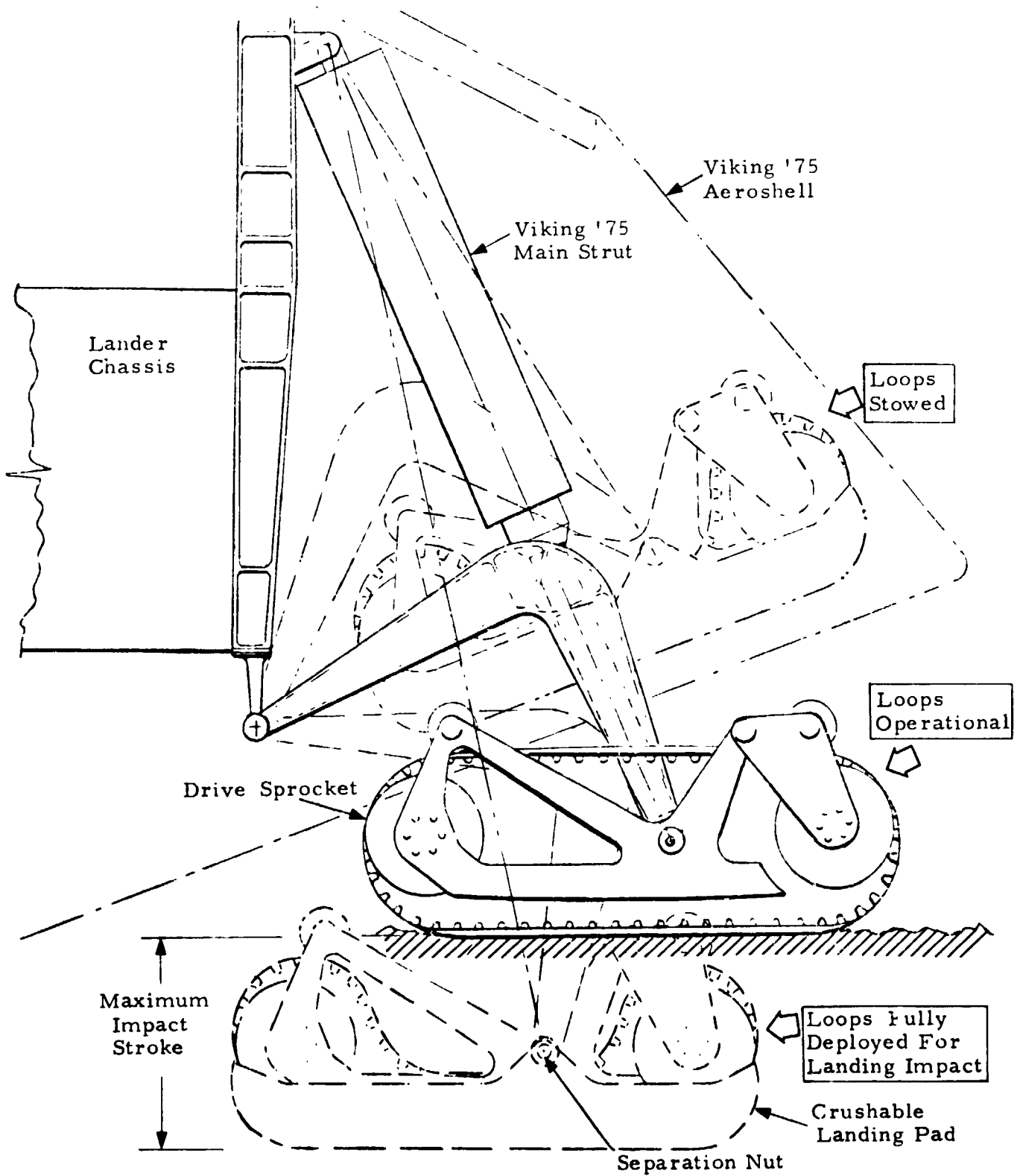


Fig. 2 - Side view of typical front loop suspension in stowed, fully deployed and cruise position.

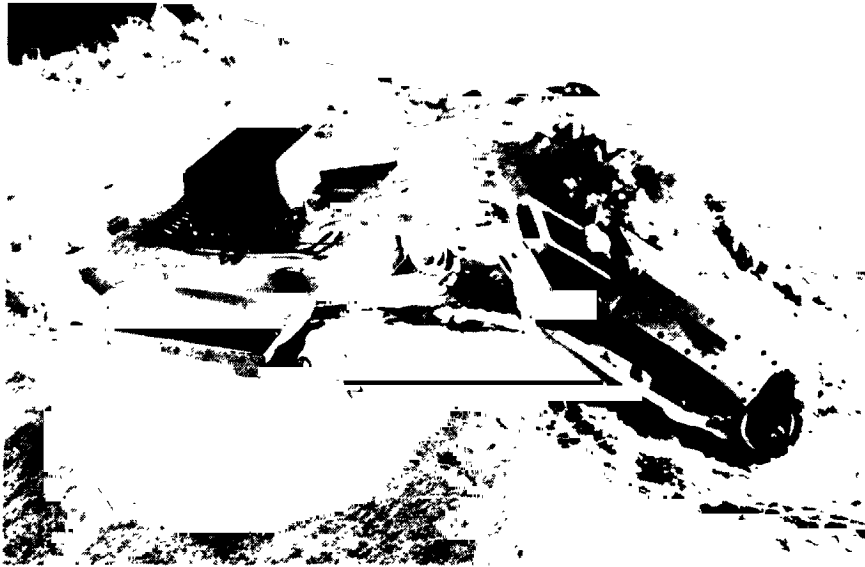


Fig. 3 - Sub-scale three-elastic-loop test vehicle with electric drive and remote control demonstrated high degree of rough-terrain mobility and maneuverability under NASA-sponsored test program.

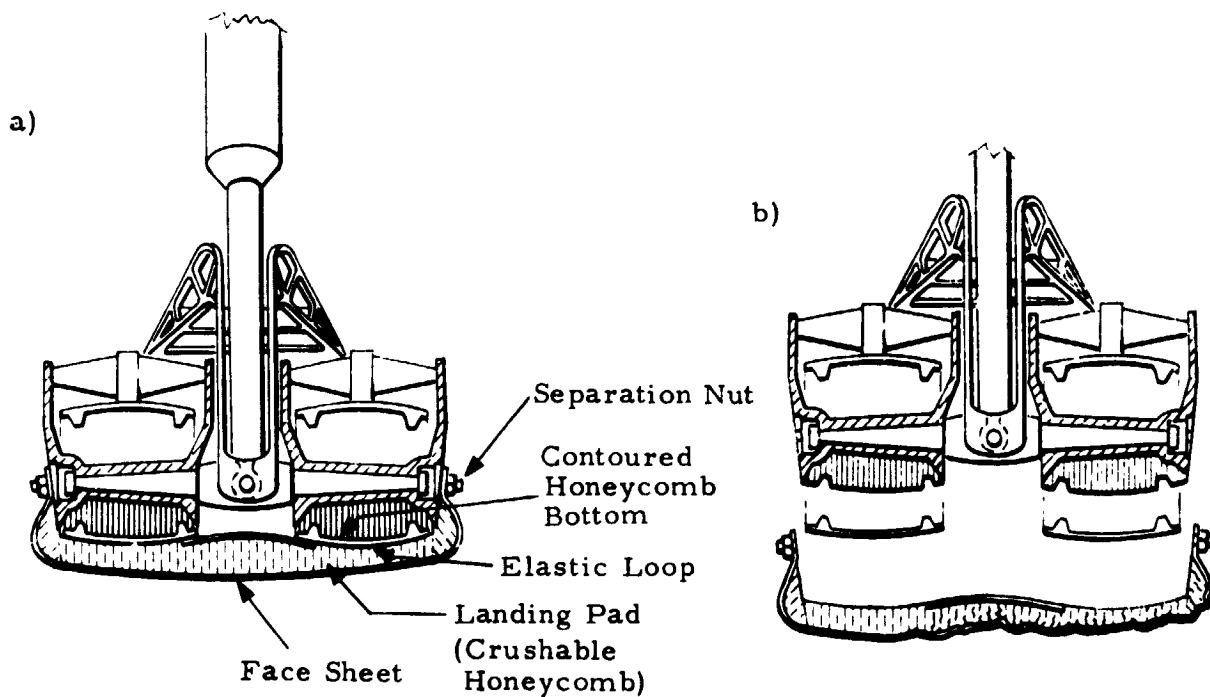


Fig. 4 - Loop protection during landing by contoured carriage bottom and crushable pad.

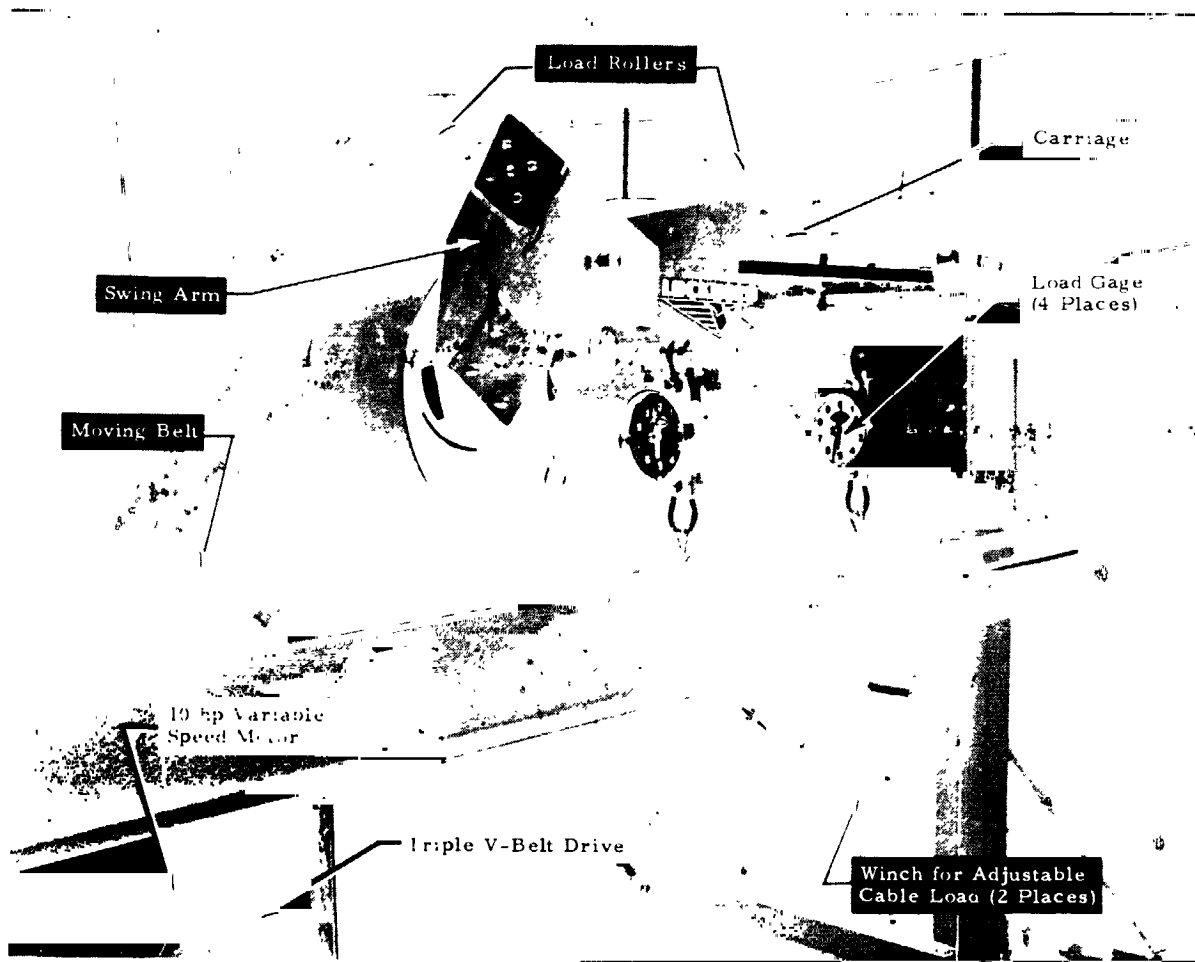
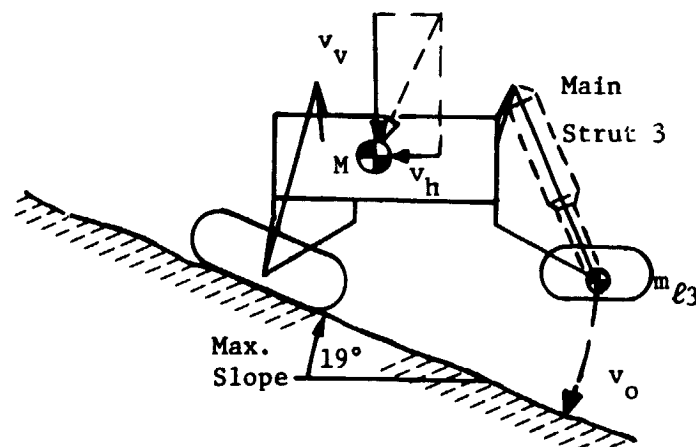


Fig. 5 - Fiberglass-epoxy test loop during endurance test on moving belt dynamometer (Ref. 12).



Worst Case:

$$v_v = 3.35 \text{ m/s}$$

$$v_h = 1.22 \text{ m/s}$$

Results In

$$v_o = 6.1 \text{ m/s At Leg 3}$$

Fig. 6 - Side view of worst case landing impact. Load peaks at leg 3 due to "slap down" motion after initial simultaneous impact of legs 1 and 2 into maximum assumed slope.

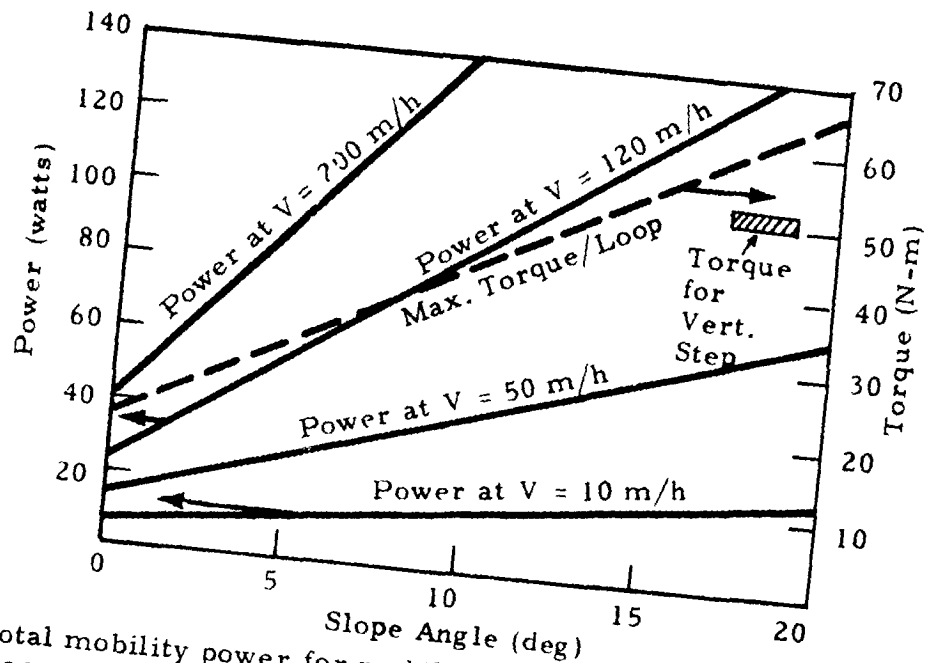


Fig. 7 - Total mobility power for mobile lander in martian loess based on loose soil tests (Ref. 8).

- Notes: 1. Assumed efficiencies were $\eta_{\text{motor/gear red.}} = \begin{cases} 0.2 & \text{at } V = 10 \text{ m/h} \\ 0.4 & \text{at } V \geq 120 \text{ m/h} \end{cases}$
 2. All power predictions multiplied by factor 1.25 to account for uncertainties and wear effects
 3. Torque prediction includes load transfer to rear loops and $\eta_{\text{gear reduction}} = 0.8$

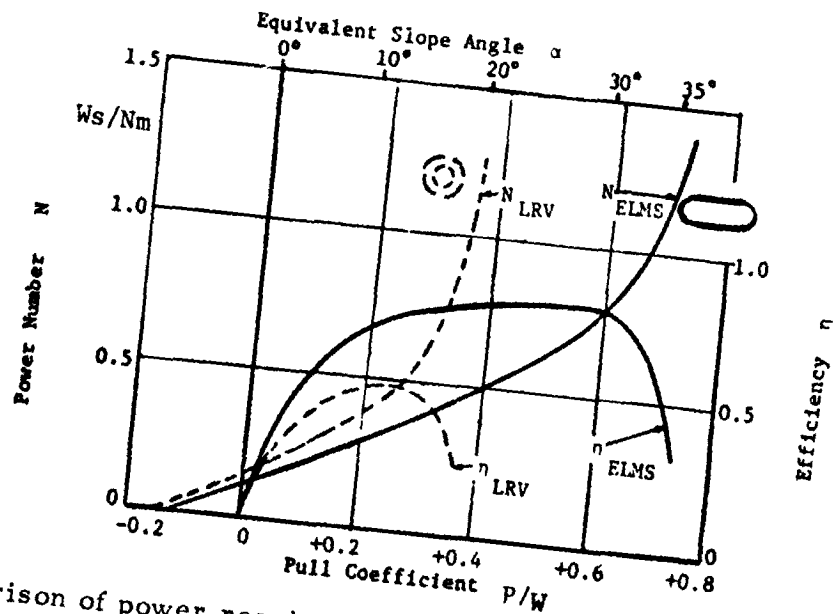


Fig. 8 - Comparison of power requirements and slope climbing capability of LRV-wheels (82 cm dia, 254 N load) and elastic loop mobility systems. "ELMS" (160 cm long, 46 cm high, 685 N load) tested in loose lunar soil simulant at WES (Refs. 8, 9); power number $N = \text{energy required (Ws) per newton load and per meter traveled}$; efficiency $\eta = \text{pull} \times \text{speed} / \text{input energy}$.

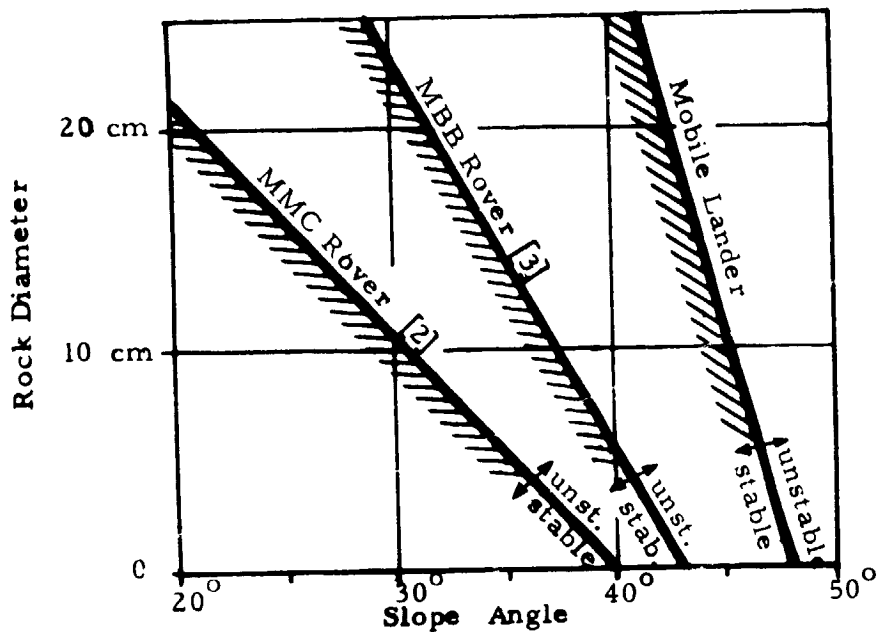


Fig. 9 - Static lateral stability boundaries for two four-wheeled rovers and mobile lander as a function of slope angle and additional rock under uphill wheels (or loops).

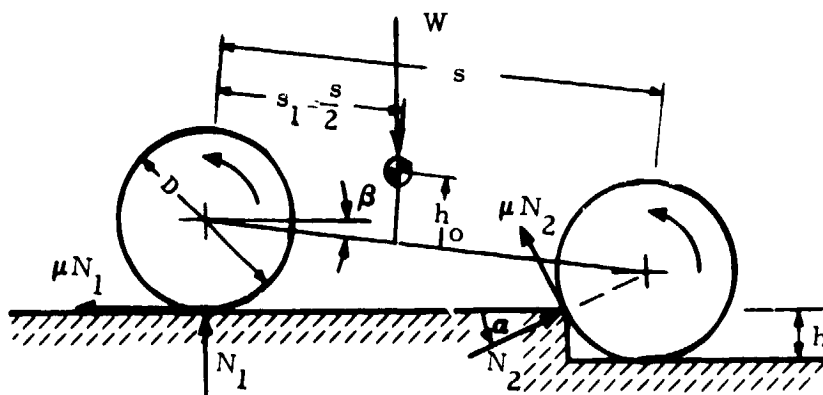


Fig. 10 - Forces acting on four-wheeled rover with all-wheel drive in critical condition for step obstacle climbing.